A pH-Dependent X-Ray Absorption Spectroscopy Study of U Adsorption to Bacterial Cell Walls

B. Ravel*, S. D. Kelly*, D. Gorman-Lewis†, M. I. Boyanov*, J. B. Fein† and K. M. Kemner*

*Biosciences Division, Argonne National Laboratory, Argonne, IL 60439, USA
†Dept. of Civil Engineering and Geological Sciences, University of Notre Dame, Notre Dame, IN 46556, USA

Abstract. Metal mobility in subsurface water systems involves the complex interaction of the metal, the fluid, and the mineral surfaces over which the fluid flows. This mobility is further influenced by metal adsorption onto bacteria and other biomass in the subsurface. To better understand the mechanism of this adsorption as well as its dependence on the chemical composition of the fluid, we have performed a series of metal adsorption experiments of aqueous uranyl $(UO_2)^{2+}$to the gram-positive bacterium *B. subtilis* in the presence and absence of carbonate along with X-ray Absorption Spectroscopy (XAS) to determine the binding structures at the cell surface. In this paper we demonstrate an approach to the XAS data analysis which allows us to measure the partitioning of the adsorption of uranium to hydroxyl, carboxyl/carbonato, and phosphoryl active sites at the cell surface.

Keywords: uranium adsorption, EXAFS
PACS: 78.70.Dm, 61.10.Ht

The failure of storage facilities containing the contaminated product of industrial, power generation, and weapons production activities has released large quantities of U and other waste products into subsurface environments, threatening water systems used for a wide variety of human activities. Accurate prediction of the fate and transport of U and other waste metals through complex, heterogeneous subsurface systems is essential for the management of waste repositories and connected water systems. [1]

The fate and transport of metals in the subsurface involves their interactions with the surrounding fluid, with the mineral surfaces over which that fluid passes, and with the biomass (such as microbial communities) present in the subsurface. The cell walls of the microbial communities present in well-populated, subsurface systems can represent a significant fraction of the total surface area exposed to the groundwater. The study of U adsorption onto bacteria, particularly at circumneutral pH conditions where U speciation is particularly complex, is ongoing.

This work involves *B. subtilis*, a common groundwater bacterium. *B. subtilis* was cultured and prepared following the procedure of Fein et al. [2, 3], including a sequence of growth, rinsing, and centrifugation. From this wet mass, solutions with known bacterial concentrations were brought to equilibrium with a U-bearing electrolyte solution. One series of samples was maintained in a closed atmosphere with CO_2 excluded. Another series was exposed to the atmosphere (and thus in equilibrium with atmospheric CO_2). A final series was open to atmosphere and reacted with a Ca-bearing electrolyte.

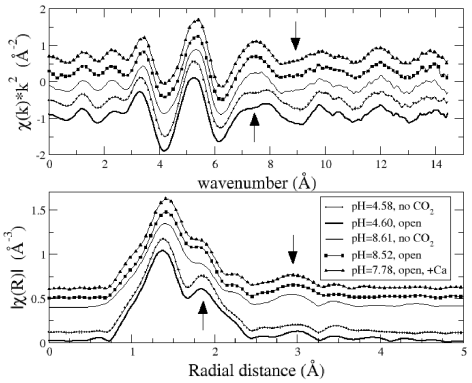

FIGURE 1. The data measured on the five samples. The arrows indicate the regions in k and R which distinguish the two groups of data, as described in the text.

U adsorption to the biomass was measured as a function of pH and modeled [3] as electrostatic interactions between the charged bacterial surface and the aqueous ion using FITEQL. [4] This model identifies multiple binding sites. From previous X-ray absorption spectroscopy (XAS) work [5, 6], these site were associated with phosphoryl and carboxyl active sites on the cell wall.

From the samples in the U adsorption studies of reference [3], five were selected for XAS measurements. Two samples at pH 4.58 and 8.61 were selected from the closed series of adsorption experiments. Two more at pH

CP882, *X-ray Absorption Fine Structure—XAFS13*
edited by B. Hedman and P. Pianetta

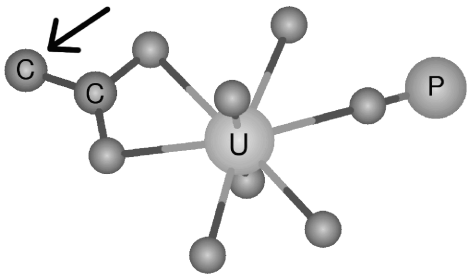

FIGURE 2. Schematic model of the structure about the U atom in this fitting model, showing an example of the phosphoryl and carboxyl ligands in the equatorial plane. The two very short axial oxygen atoms are shown extending into and out of the page. The atom marked with an arrow would be an oxygen in the case of a carbonato complex.

4.60 and 8.52 were chosen from the series in equilibrium with the atmospheric CO_2. One sample at pH=7.78 was taken from the series with added Ca. The paste from the centrifuged samples, with approximately 400 ppm U on the biomass, was placed in sample containers and sealed from contact with the air by kapton film. They were measured in transmission at the MRCAT [7] beamline at the Advanced Photon Source. These data. shown in Figure 1, are more sensitive to pH than to the presence of CO_2 or Ca. The arrows in the figure indicate the distinctive regions in k and R distinguishing the low pH data from the high.

CONSTRAINTS AND RESTRAINTS

Adsorption experiments like those described in references [2] and [3] are significant in the study of the uranium/bacterium interaction. However they cannot uniquely identify the adsorption complex nor can they directly determine how much of the adsorption is due to each complex. XAS provides a direct measure of the average structural environment around the uranium atoms, thus nicely compliments the adsorption measurements.

As in reference [5], we expect the uranium to be bound to phosphoryl and carboxyl ligands and with bare oxygen atoms (which could be associated with a hydration shell or with a hydroxyl ligands, which are probably impossible to distinguish in our measurements). In our analysis of the extended x-ray-absorption fine-structure (EXAFS) data, we want to allow for the partitioning of the U absorber onto each of these ligands. In the most simple-minded approach to EXAFS data analysis, the parameters of the EXAFS equation — N, S_0^2, E_0, ΔR, and σ^2 — are the variables of the fit. Floating N and ΔR independently for each kind of scatterer would introduce a statistically insupportable number of parameters into the fit. Instead, we use the capability of IFEFFIT [8, 9] to describe abstract structural models through the use of constraints and restraints on the parameters refined in the fit.

TABLE 1. (top) Partitioning of equatorial oxygens among the ligands considered in this fitting model. (bottom) Distances to the various scatterers.

pH	CO_2	Phosphryl	Carboxyl	Bare O
4.60	yes	2.13(17)	1.18(78)	2.69(79)
4.58	no	2.36(17)	1.19(84)	2.45(86)
7.78	yes	3.50(19)	0.96(86)	1.54(88)
8.61	no	3.78(25)	1.78(1.24)	0.44(1.26)
8.52	yes	3.44(19)	0.59(82)	1.96(83)

O	R (Å)	other	R (Å)
axial	1.772(4)	P	3.578(16)
short	2.270(9)	C	2.931(36)
long	2.424(8)	Na	4.014(28)

Constraint An assertion about the value of a fitting parameter or a fixed relation between two or more parameters used in the fit.

Restraint An expression placing a soft limit on the range of values available to one or more fitting parameters. The restraint is added in quadrature to the χ^2 fitting metric.

Uranyl phosphate and uranyl carbonate standards were calculated using FEFF6 [10], following the approach of reference [5]. Uranyl species commonly have two axial O atoms at about 1.78 Å and a number of equatorial oxygen atoms. When the number of equatorial O atoms was allowed to float, it consistently refined to 6 (within uncertainty). For the fits reported here, the number was fixed to 6. Those six atoms were then partitioned among the various ligand types.

This guided our approach to modeling these data. Because phosphorous coordinates to U via a monodentate O bridge with a U–O distance of ∼2.28 Å, the number of phosphorous scatterers is constrained to equal the number of short equatorial oxygen atoms. Carbon – either as a carboxyl ligand or an inorganic carbonato complex – coordinates U via longer, bidentate O bridge with U–O distance of ∼2.43 Å, hence the number of carbon scatterers is restrained not to exceed half the number of long equatorial oxygen atoms. Any long equatorial oxygens in excess of twice the number of carbon scatterers are interpreted as bare oxygen atoms. Both the phosphoryl and carboxyl ligands contribute nearly collinear multiple scattering paths whose numbers are constrained by the numbers of single scattering paths. The remainder of the parameters used in the fit used typical constraints. For example, the the axial oxygens were constrained to have the same ΔR and σ^2 regardless of equatorial lig-

ation. As another example, the data did not support independent measurements of σ^2 for the short and long equatorial oxygen atoms, so all equatorial oxygen paths were constrained to have the same σ^2 in the fit. A complete description of the fitting model will be provided in an upcoming publication. The result of this fitting model is shown in Figure 3 for the pH=8.52 sample exposed to atmosphere. The other fits were of comparable quality.

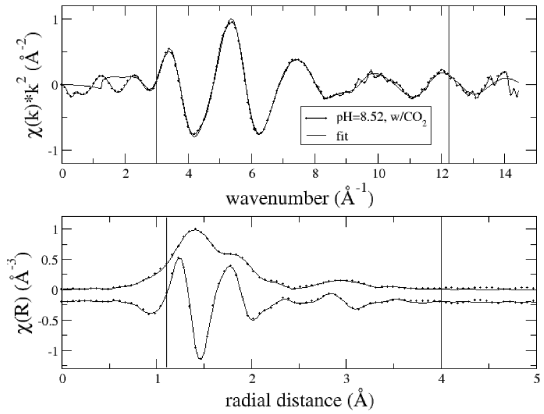

FIGURE 3. Fit to the sample of U adsorbed to *B. subtilis* at pH=8.52 and exposed to atmosphere. The vertical lines indicate the Fourier transform range in k and the fitting range in R. The bottom panel shows the magnitude of $\tilde{\chi}(R)$ along with the real part displace vertically for clarity.

U ADSORPTION TO *B. SUBTILIS*

These EXAFS results fit well within the context of the adsorption results of reference [3]. As with the earlier EXAFS results [5], we see a decrease in binding to phosphoryl sites with increasing pH. The adsorption results are consistent with the formation of a uranyl carbonate complex on the cell wall at higher pH. In principle, an EXAFS measurement can distinguish between the organic carboxyl ligand and the inorganic carbonato complex. From the perspective of the U absorber, the difference between these two species is the distance between the U absorber and the atom marked by the arrow in Fig. 2. A carbonato has the same bidentate oxygen bridge between the U and C atoms, however the C atom at about 4.35 Å is replaced by an O atom at about 4.20 Å. Whether these data can distinguish between the two species, given the paucity of spectral weight beyond 3.5 Å in these data and the relative weakness of O and C as a scatterer, is a matter of further investigation.

There is one discrepancy between our results shown in Table 1 and the thermodynamic modeling of reference [3]. In that reference, the addition of calcium to the U–*B. subtilis* parent solution resulted in the adsorption data that could only be modeled by the addition of a calcium uranyl carbonate surface complex. Our fit to the pH=7.78 data containing both CO_2 and added Ca is not consistent with the presence of a Ca scatterer. Rather, to obtain fits of the quality shown in Figure 3, we added a Na scatterer at about 4 Å — the approximate position expected for a Ca scatterer in calcium uranyl carbonate. Work is ongoing to resolve this issue.

ACKNOWLEDGMENTS

Much of this work was supported by the Environmental Remediation Science Program, Office of Biological and Environmental Research, Office of Science, U.S. Department of Energy. Use of the Advanced Photon Source was supported by the U. S. Department of Energy, Office of Science, Office of Basic Energy Sciences, under Contract No. W-31-109-ENG-38. The Materials Research Collaborative Access Team (MRCAT) operations are supported by DOE and the MRCAT member institutions. Additional support by the National Science Foundation through an Environmental Molecular Science Foundation grant (EAR02-21966).

REFERENCES

1. A NABIR Primer, Bioremediation of Metals and Redionuclides: What it is and how it works, Tech. Rep. second edition, Office of Biological and Environmental Research, Office of Science, U.S. Department of Energy (2003).
2. J. Fein, C. Daugheny, N. Yee, and T. Davis, *Geochim. Cosmochim. Acta* **61**, 3319–3328 (1997).
3. D. Gorman-Lewis, P. Elias, and J. Fein, *Environ. Sci. Technol.* **39**, 4906–4912 (2005).
4. A. Herbelin, and J. Westall, Fiteql 4.0: a computer program for determination of chemical equilibrium constants from experimental data, Tech. Rep. 99-01, Department of Chemistry, Oregon State University, Corvallis OR (1999).
5. S. Kelly, K. Kemner, J. Fein, D. Fowle, M. Boyanov, B. Bunker, and N. Yee, *Geochim. Cosmochim. Acta* **66**, 3875–3891 (2002).
6. M. Boyanov, S. Kelly, K. Kemner, B. Bunker, J. Fein, and D. Fowle, *Geochim. Cosmochim. Acta* **67**, 3299–3311 (2003).
7. C. Segre, N. Leyarovska, L. Chapman, W. Lavender, P. Plag, A. King, A. Kropf, B. Bunker, K. Kemner, P. Dutta, R. Duran, and J. Kaduk, "The MRCAT insertion device beamline at the Advanced Photon Source," in *Synchrotron Radiation Instrumentation: Elebenth U.S. Conference*, 2000, vol. CP521, pp. 419–422.
8. M. Newville, *J. Synchrotron Radiat.* **8**, 322–324 (2001).
9. B. Ravel, and M. Newville, *J. Synchrotron Radiat.* **12**, 537–541 (2005).
10. S. I. Zabinsky, J. J. Rehr, A. Ankudinov, R. C. Albers, and M. J. Eller, *Phys. Rev. B* **52**, 2995–3009 (1995).